Frontiers in Computing and Intelligent Systems
ISSN: 2832-6024 | Vol. 3, No. 1, 2023

Research on Beidou Navigation Interference Monitoring Technology Based on CFAR

Xiaodong Zhang, Benlei Su

College of Electronic and Information, Southwest Minzu University, Chengdu, China.

Abstract: Satellite monitoring stations are often affected by strong clutter and interference when monitoring targets. When ground receivers receive target signals, they also receive noise, clutter, and interference signals. These signals have randomness and signal strength changes from time to time. Therefore, constant false alarm detection technology is used to detect interference signals. CFAR detectors construct different system functions in different clutter environments and maintain a constant false alarm rate by adaptively modifying the detection threshold. A comparison of CFAR algorithms shows that CA_ The CFAR algorithm has excellent monitoring performance in uniform environments_ CFAR is suitable for multi target environments, GO_ CFAR performs well in clutter edge environments, SO_ CFAR performs well under various conditions.

Keywords: Satellite navigation; Interference monitoring; MATLAB; CFAR; Constant false alarm detection.

1. Introduction

China's BeiDou Navigation Satellite System (BDS) is a global satellite navigation system developed by China itself. It consists of three parts: satellite, ground station, and user positioning equipment. The ground station is responsible for transmitting signals to the satellite and receiving signals transmitted by other ground stations through the satellite. In the process of receiving signals, mutual interference between various signals and some intentional and unintentional human interference [1 have a significant impact on the normal operation of the satellite navigation system. How to quickly and accurately detect interference signals is a difficult problem.

In relevant research, Lei Liang [4] adopted a dual threshold threshold decision method and threshold cyclic updating to reduce the missed alarm rate and false alarm probability. Guo Xuqiang [5] proposed an interference frequency point detection algorithm based on Rayleigh mean characteristics, which does not require detection threshold iteration and update, and has a detection probability equivalent to the FCME algorithm at an interference to noise ratio above 40dB. Huang Ting [6] proposed a large dynamic AGC algorithm based on amplitude limiting ratio, which utilizes the effective bit number of single frequency interference to minimize the signal-to-noise ratio of the input signal after quantization. This algorithm can adapt to different interference types and ensure reception performance under different interference styles. Jim é nez et al. [7] conducted a performance analysis of the general unit average constant false alarm rate (CA-CFAR) in a uniformly Weibull distributed clutter environment, providing general expressions for detection probability (PD) and false alarm probability (PFA), which allow the shape parameters of Weibull interference to have arbitrary values. Sahal et al. [8] evaluated the detection performance of four CFAR algorithms in terms of detection rate and processing time, proving that OS-CFAR has the best detection performance, but its processing time is slightly longer than other algorithms. Smith et al. [9] proposed a method to distinguish different backgrounds based on the statistical characteristics of mean and variance. Select CA-CFAR, SO-CFAR, or GO-CFAR for processing based on different background characteristics. In a uniform background, CFAR has a small detection loss, can effectively detect multiple targets, and can control false alarms at the edge of clutter.

This article describes the common interference in satellite navigation systems, and analyzes the SO in different clutter environments_ CFAR、GO_ CFAR、OS_ CFAR and CA_ The detection performance of CFAR algorithm can be used to determine which algorithm can achieve the highest detection rate in different backgrounds.

2. Interference Classification and Modeling of Beidou Satellite Navigation System

2.1. Interference classification

The interference received by satellite navigation receivers can generally be divided into two categories: deception interference and suppression interference. The structure diagram is as follows. When the receiver receives satellite signals, suppressed interference can cause the receiver to receive many clutter signals. The CFAR algorithm can distinguish useful target signals in the clutter background, so this article focuses on monitoring suppressed interference.

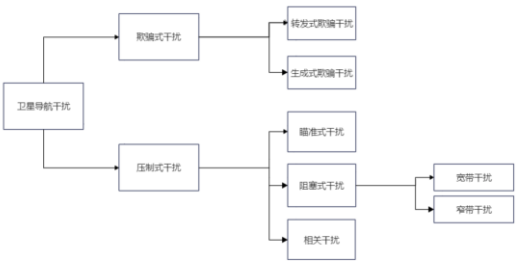

Figure 1. Structure Diagram of Satellite Navigation Jamming

2.2. Modeling and Analysis of Suppressive Interference

Suppressive jamming refers to the jamming device that emits a high-power interference signal to interfere with the satellite navigation receiver. The frequency point of the interference signal is the same as or within the frequency band of the satellite navigation system. This high strength signal

can cause the real satellite navigation signal to be buried, thereby forming interference. The disadvantage of this method is that the power required for the broadcast interference signal is very high. When the distance is too far and the antenna gain is insufficient, it is difficult to generate such a signal. However, due to the unique characteristics of navigation signals, suppression jamming has advantages over other jamming methods. At the same time, general suppression jamming is used to interfere with C/A codes.

In terms of signal generation methods, suppression interference can be divided into Gaussian white noise interference, audio interference, frequency sweep interference, pulse interference, and BPSK interference.

2.2.1. Gaussian white noise

The main noise encountered by navigation receivers is thermal noise. At room temperature, thermal noise can be considered as Gaussian white noise with a power spectral density N of - 174 dBm/Hz, with a statistical mean of 0 and a statistical variance of 1. Figure 2 is the time domain waveform of Gaussian white noise, Figure 3 is the normalized power spectrum of Gaussian white noise, and Figure 4 is the amplitude frequency histogram of Gaussian white noise. It can be seen that the amplitude frequency histogram of Gaussian white noise follows a normal distribution.

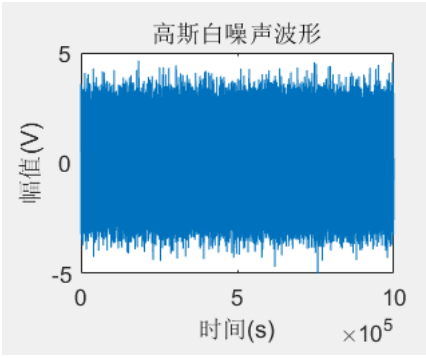

Figure 2. Time Domain Waveform of Gaussian White Noise

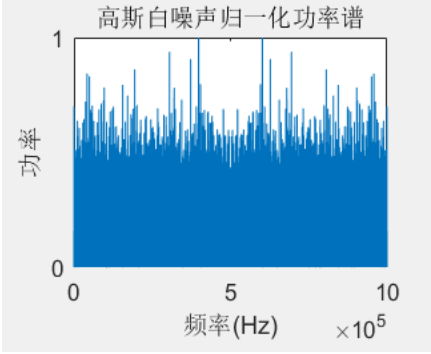

Figure 3. Normalized Power Spectrum of Gaussian White Noise

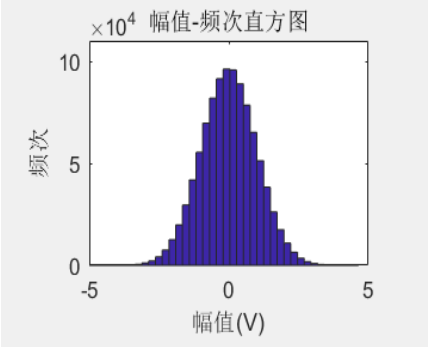

Figure 4. Amplitude Frequency Histogram of Gaussian White Noise

2.2.2. Audio interference

Audio interference is divided into single tone interference (CWI) and multi tone interference (SCWI). Single tone interference belongs to targeted interference, which only involves interference at one frequency point on the navigation signal, and the interference power at other frequency points is 0. The characteristics are: continuous in time domain, and single tone in frequency domain. Multi tone interference forms impulses at certain frequency points within the navigation frequency band, consisting of multiple single tone interference.

The formula for a single tone signal is

$$J(t) = U_j \sin(2\pi f_j t + \varphi) \quad (1)$$

Where, $U_j$is the amplitude of a single tone, f_j is a single tone frequency, φ at [0,2 π]Uniformly distributed within a single tone signal with only one spectral line.

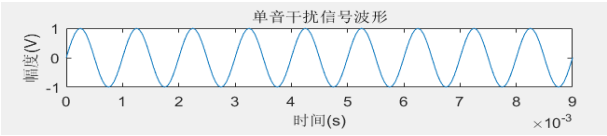

Figure 5. Waveform of Monotone Interference Signal

Figure 6. Normalized Power Spectrum of Monotone Interference Signal

A multitone signal is generated by superposition of L independent sinusoidal signal waveforms. The multitone signals simulated by MATLAB are 940Hz, 960Hz, 980Hz, 1000Hz, 1020Hz, 1040Hz, 1060Hz, L=7.

The formula for multitone signals is

$$J(t) = \sum_{n-1}^{L} U_{jn} \sin(W_n t + \varphi_n) \quad (2)$$

among $W_n = 2\pi(f_j + n\Delta f)$, f_j is the multi tone starting frequency, Δf is the multi tone interval frequency, and the frequencies of the nth and sinusoidal signals are $f_j + n\Delta f$ multitone signal has $*L*$ root frequency line.

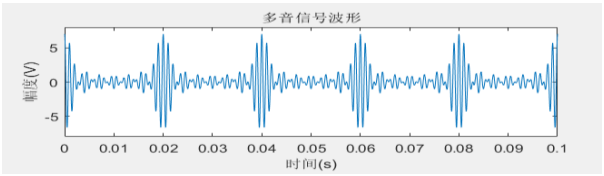

Figure 7. Multitone Signal Waveform Diagram

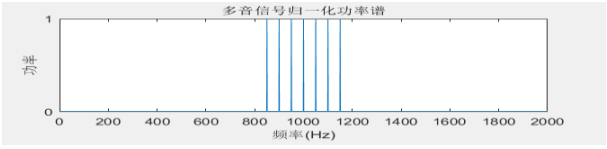

Figure 8. Normalized power spectrum of multitone signal

2.2.3. Linear swept frequency interference

Linear swept frequency (LFM) signals mainly modulate the carrier frequency in order to obtain a larger transmission bandwidth and achieve pulse compression during reception. In the Beidou navigation system, linear swept frequency interference is the most common time-varying suppressed interference, whose instantaneous frequency varies linearly with time.

The formula for a linear sweep signal is

$$u(t) = Arect(\frac{t}{T})cos[2\pi(f_0 t + \frac{1}{2}ut^2)] \quad (3)$$

The instantaneous frequency of a linear sweep signal is

$$f(t) = f_0 + ut(u = \frac{f_1 - f_0}{T}) \quad (4)$$

Where, f_0 is the starting frequency, f_1 is the termination frequency. U is the sweep slope. This simulation selects a linear sweep signal with a starting cutoff frequency of 5Hz and a scan slope of 95Hz/s.

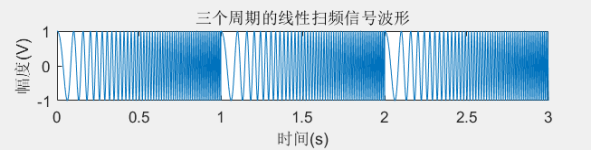

Figure 9. Three Periodic Linear Sweep Waveforms

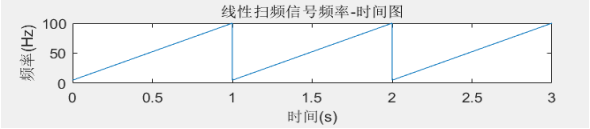

Figure 10. Frequency Time Diagram of Linear Sweep Signal

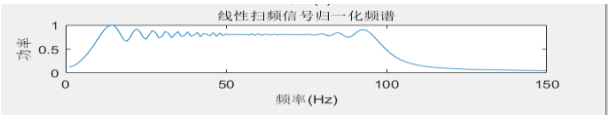

Figure 11. Normalized Spectrum of Linear Sweep Signal

2.2.4. Single frequency pulse interference

Pulse interference (PI) consists of irregular pulses with a short duration, mainly from man-made industrial interference. Its single pulse has a short duration and a large time interval between adjacent pulses, often having a wide spectrum, extending from low frequency to high frequency. The higher the frequency, the lower the energy.

Pulse jamming $S(t)$ the time function of is

$$S(t) = \begin{cases} Ae^{j2\pi f_0 t, 0\in[0,T]} \\ 0, others \end{cases} \quad (5)$$

Using Euler's formula

$$e^{ix} = cosx + isinx \quad (6)$$

So the real part of the time function of CW can also be written

$$S(t) = Acos(2\pi f_0 t) \quad (7)$$

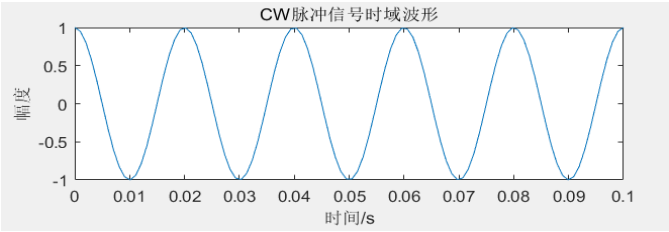

Figure 12. Time Domain Waveform of CW Pulse Signal

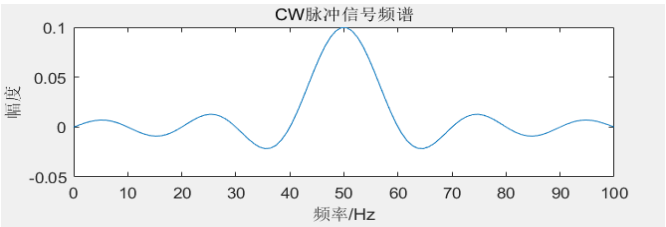

Figure 13. CW pulse signal spectrum

3. Interference monitoring technology

The commonly used interference monitoring techniques include fixed threshold method and adaptive threshold method. The fixed threshold method refers to the detection of signals when the signal received by the receiver is greater than the fixed threshold value, but in daily life, there are often scenes with strong interference signals. For example, unmanned aerial vehicles (UAVs) are often in a clutter environment during flight patrols, with multiple interference signals, and if they continue to use the fixed threshold value at this time, the false alarm rate will greatly increase. Therefore, in this case, a constant false alarm rate (CFAR) detector is used. The constant false alarm rate (CFAR) detector maintains a constant false alarm rate by adaptively modifying the detection threshold, and maximizes the detection probability.

The constant false alarm detector includes unit average CFAR (CA-CFAR), minimum CFAR (SOCA-CFAR), maximum CFAR (GOCA-CFAR), and ordered statistical CFAR (OS-CFAR). The difference between different CFAR detectors lies in how to construct the statistical functions of the system.

3.1. Introduction to Common CFAR Algorithms

(1) CA_ CFAR

Cell average (CA) - CFAR is the most commonly used constant false alarm detection algorithm

Excellent detection performance in environments, but significant loss of detection performance in multi target and clutter edge environments. This calculation

The method uses the mean value of the adjacent sliding window echo data of a single frame of the unit to be detected as a reference value for background clutter power

Y. The specific calculation formula is as follows

$$Y = \frac{1}{N}\sum_{i=1}^{N} x_i \quad (8)$$

"N is the reference sliding window length, xi is the echo data of the adjacent sliding window of the unit to be detected, and Y is the back"

Background clutter power reference value. The detection threshold T can be deduced as

$$T = \alpha * Y = \frac{a}{N}\sum_{i=1}^{N} x_i \quad (9)$$

Because the detection threshold T is a numerical fluctuation that occurs as the average value of the sliding window changes as the unit to be detected approaches

So the false alarm probability expectation can be solved by the simultaneous integration of the above equation. The formula is as follows

$$\overline{PFA} = \int_0^{\infty} exp(-\frac{T}{\gamma})f(T)dT$$
$$= \frac{1}{(N-1)!}(\frac{1}{\beta\gamma})^N \int_0^{\infty} T^{N-1} exp(-\frac{(1+\beta)T}{\beta\gamma})dT \quad (10)$$

The expected value of false alarm probability obtained through partial integration is

$$\overline{PFA} = (1+\beta)^{-N}$$
$$= (1+\frac{\alpha}{N})^{-N} \quad (11)$$

When the preset false alarm probability PFA is known, the threshold factor can be inversely derived from the above formula α by

$$\alpha = N(PFA^{-\frac{1}{N}} - 1) \quad (12)$$

(2) SO_ CFAR

Smallest Of (SO) - CFAR is a mean CFAR algorithm that has been developed to address the increase in false positives from CA-CFAR in a multi target environment. The real purpose of this algorithm is to eliminate the masking effect caused by interfering targets in the reference window. If an interfering target appears in one of the leading and lagging parts, the estimated noise level parameters for that part will be increased. Its background clutter power reference value Y the calculation formula is as follows

$$Y = \min(A, B) \tag{13}$$

False Alarm Probability PFA and Threshold Factor of SO-CFAR α the relationship is as follows

$$PFA = 2\sum_{i=0}^{N/2-1}\binom{N/2+i-1}{i}\left(2+\frac{a}{N/2}\right)^{-(N/2+i)} \tag{14}$$

(3) GO_ CFAR

Greatest Of (GO) - CFAR is a mean CFAR algorithm developed to address the increased false alarms of CA-CFAR in clutter edge environments. This algorithm divides the reference window around the notch into leading and lagging parts, calculates the average of the two parts, and compares the results. The calculation formula for the background clutter power reference value Y is as follows

$$Y = \max(A, B) \tag{15}$$

A is the average value of the front half sliding window of the unit to be tested, and B is the average value of the rear half sliding window of the unit to be tested.

The False Alarm Probability PFA of GO-CFAR and the Threshold Factor α the relationship is as follows

$$PFA = 2\left(1+\frac{a}{N/2}\right)^{-N/2} - 2\sum_{i=0}^{N/2-1}\binom{N/2+i-1}{i}\left(2+\frac{a}{N/2}\right)^{-(N/2+i)} \tag{16}$$

(4) OS_ CFAR

OS-CFAR has excellent detection performance in multi target environments, but its performance has some losses in uniform environments and clutter edge environments. OS-CFAR needs to sort the adjacent sliding window data of the unit to be detected in a single frame, and use the ranked k-th largest echo data as its background clutter power reference value Y. The value of k is determined by the proportional value rate, which is generally set to 0.75. The specific calculation formula is as follows

$$k = rate * N \tag{17}$$

False Alarm Probability PFA and Threshold Factor of OS-CFAR α the relationship is as follows

$$PFA = k\binom{N}{k}\frac{\tau(N-K+1+\alpha)\tau(k)}{\tau(N+1+\alpha)} \tag{18}$$

The following will apply to the CA_ CFAR is compared with the other three algorithms.

3.2. CA_ CFAR and SO_ CFAR

When there is a strong interfering target in the reference range unit, the CA-CFAR detection threshold will increase, making it difficult to detect targets with weak signals.

The threshold calculation at the distance unit in Figure 14 is based on the distance unit as the center, and the left and right sides are used as reference units. Due to the strong targets included in the reference unit of the weak target in the figure, the threshold calculation at the weak target is too large, resulting in missed detection; Figure 15 SO used_ The CFAR detector calculates the average clutter power of the left and right reference range units separately, and takes the smaller estimate as the average clutter power of the range unit to be detected to calculate the detection threshold to avoid missing weak targets.

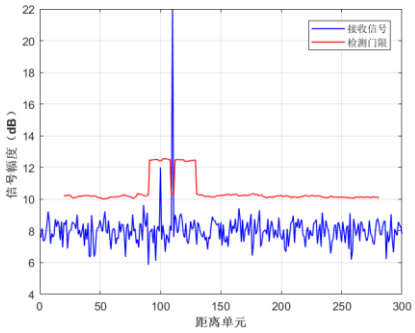

Figure 14. CA-CFAR Detector

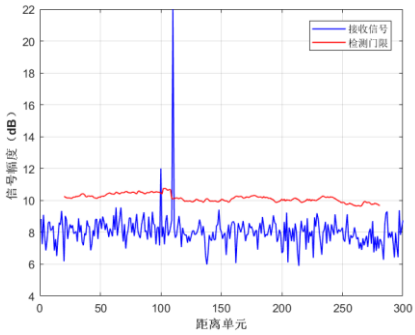

Figure 15. SO-CFAR Detector

3.3. CA_ CFAR and GO_ CFAR

When using the CA-CFAR detection algorithm under uneven clutter conditions, the false alarm rate will greatly increase at the edge of the clutter.

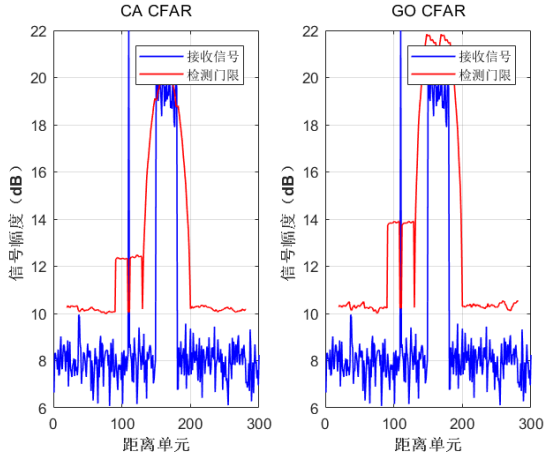

Figure 16. CA-CFAR Detector **Figure 17.** GO-CFAR Detector

In Figure 16, the clutter amplitude value at some distance units is relatively large, exceeding the threshold, leading to false alarms; Figure 17 uses GO_ CFAR calculates the average clutter power of the left and right reference units separately, and takes the larger estimated value as the average clutter power of the distance unit to be detected to calculate the detection threshold, avoiding the occurrence of false alarms.

3.4. CA_ CFAR and OS_ CFAR

When there are multiple strong interference targets in the reference unit, the presence of multiple targets can cause the estimated average clutter power to be too high, thereby raising the detection threshold and causing missed alarms.

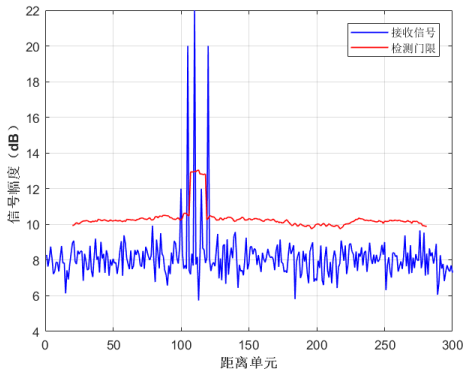

Figure 18. CA-CFAR Detector

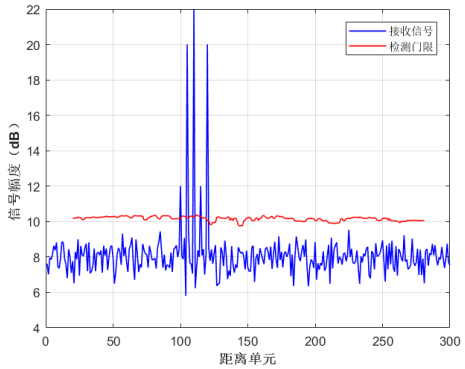

Figure 19. OS-CFAR Detector

Figure 19 ranks the echo power of each reference range unit, selecting a value in the middle as the average clutter power of the range unit to be detected to calculate the threshold.

4. Conclusion

This paper studies satellite navigation interference monitoring technology, describes the main types of interference in satellite navigation systems, and conducts modeling and simulation for common suppressed interference signals, laying a foundation for interference target identification and interference monitoring algorithm research in the interference monitoring process. Different algorithms are used to detect different clutter environments. By comparing the detection performance, it is concluded that using CA in a uniform environment_ CFAR algorithm is sufficient, SO_ CFAR and GO_ CFAR is suitable for multi target environments and clutter edge environments, respectively_ CFAR performs well in various noise backgrounds. However, this algorithm has a high complexity and a long calculation time, so it is necessary to accelerate the calculation process of the threshold in the CFAR algorithm. It can integrate machine learning and deep learning algorithms to speed up the processing time.

Acknowledgments

This work was financially supported by Southwest University for Nationalities Graduate Innovative Research Project (YB2022829) fund.

References

[1] Huang Lei, Ma Wenjia. Research and Analysis of Satellite Navigation Interference Monitoring Technology [J]. China Integrated Circuit, 2021,30 (07): 12-16+49.

[2] Fan Guangwei, Chao Lei, Liu Li. Satellite navigation interference monitoring technology [J]. Journal of Sichuan Military Industry, 2013,34 (06): 16-79.

[3] Han Qiwei, Zeng Xianghua, Li Zhengrong, et al Development Status and Trend of Satellite Navigation Interference Monitoring Technology [J] Aerospace Electronic Countermeasures, 2009 (6): 4.

[4] Lei Liang Research on interference monitoring technology for GNSS satellite navigation system [D]. Gansu: Lanzhou Jiaotong University, 2017.

[5] Guo Xuqiang Research on Beidou Satellite Navigation Interference Detection and Identification Technology [D]. Beijing: Beijing Jiaotong University, 2018.

[6] Huang Ting Research on Key Technologies of Suppressive Interference Monitoring for Satellite Navigation Systems [D]. Hunan: Hunan University, 2014.

[7] Jiménez L P J, García F D A, Alvarado M C L, et al. A General CA-CFAR Performance Analysis for Weibull-Distributed Clutter Environments[J]. IEEE Geoscience and Remote Sensing Letters, 2022.

[8] Sahal M Said Z A , Putra R Y , et al. Comparison of CFAR Methods on Multiple Targets in Sea Clutter Using SPX-Radar-Simulator[C]// 2020 International Seminar on Intelligent Technology and Its Applications (ISITIA). IEEE, 2020.

[9] Smith M E, Varshney P K . Intelligent CFAR processor based on data variability[J]. IEEE Transactions on Aerospace & Electronic Systems, 2002, 36(3):837-847.

[10] Hatem G M, Saeed T R , Sadah J . Comparative Study of Combined CFAR Algorithms for Non-Homogenous Environment [J]. Procedia Computer Science, 2018, 131:58-64.

[11] Wang Z , He Z , He Q , et al. Adaptive CFAR Detectors for Mismatched Signal in Compound Gaussian Sea Clutter With Inverse Gaussian Texture[J]. IEEE Geoscience and Remote Sensing Letters, 2021, PP (99):1-5.